PORTLAND PRESS

Review Article

Elastic and thermodynamic consequences of lipid membrane asymmetry

Samuel L. Foley¹, Malavika Varma¹, Amirali Hossein² and ¹ Markus Deserno¹

¹Department of Physics, Carnegie Mellon University, Pittsburgh, PA 15213, U.S.A.; ²NIH (National Institutes of Health), NICHD (Eunice Kennedy Shriver National Institute of Child Health and Human Development), Eunice Kennedy Shriver National Institute of Child Health and Human Development, Bethesda, MD, U.S.A.

Correspondence: Markus Deserno (deserno@andrew.cmu.edu)

Many cellular lipid bilayers consist of leaflets that differ in their lipid composition — a non-equilibrium state actively maintained by cellular sorting processes that counter passive lipid flip-flop. While this lipidomic aspect of membrane asymmetry has been known for half a century, its elastic and thermodynamic ramifications have garnered attention only fairly recently. Notably, the torque arising when lipids of different spontaneous curvature reside in the two leaflets can be counterbalanced by a difference in lateral mechanical stress between them. Such membranes can be essentially flat in their relaxed state, despite being compositionally strongly asymmetric, but they harbor a surprisingly large but macroscopically invisible differential stress. This hidden stress can affect a wide range of other membrane properties, such as the resistance to bending, the nature of phase transitions in its leaflets, and the distribution of flippable species, most notably sterols. In this short note we offer a concise overview of our recently proposed basic framework for capturing the interplay between curvature, lateral stress, leaflet phase behavior, and cholesterol distribution in generally asymmetric membranes, and how its implied signatures might be used to learn more about the hidden but physically consequential differential stress.

Introduction

Lipid membranes enclose all living cells and form many distinct functional compartments in eukaryotic cells [1, 2]. Their basic architecture is that of a bilayer — a structure in which two lipid leaflets
appose one another such that their hydrophobic tails are 'tucked away' on the inside. There is no
reason why these two leaflets would have to be identical in every respect, and work starting in the
1970s showed that they indeed differ in composition for (at least) the plasma membrane of many cell
types [3–6]. More recent work has increased the resolution of this leaflet-specific lipidomic fingerprint
and argued, using a proteomic signature and tools from bioinformatics, that it seems evolutionarily
conserved across all of eukarya [7].

The existence of a leaflet-specific lipidome has become known as *membrane asymmetry*, but of course the notion of 'asymmetry' encompasses more than lipid identity: as long as the two leaflets differ in at least one physical parameter, the reflection symmetry of a membrane with respect to its midplane breaks down, with potentially many interesting consequences. Observe that this might happen even if both leaflets consist of the *same* lipids; for instance: (i) different peripheral proteins might be attached on both sides; (ii) ionic conditions and/or pH might differ across the membrane, which could affect the lipids' protonation state on either side and hence the membrane's surface charge density and (iii) lipids could be packed at unequal densities, which in turn would lead to a different state of lateral stress in each leaflet.

The possibility that differential stress in lipid membranes might not just exist but in fact be ubiquitous and even responsible for intriguing new phenomena has been increasingly recognized in recent years [8–14], including the realization that this poses new challenges for simulations [15–22]. While it can arise

Received: 31 October 2022 Revised: 2 February 2023 Accepted: 10 February 2023

Version of Record published: 7 March 2023



in a bilayer comprising just a single lipid species, many of its interesting features arise as an interplay with other aspects of bilayer physics, such as composition-induced spontaneous curvature, the fluid–gel phase transition, and cholesterol partitioning between leaflets. We will examine some of the resulting consequences in this short note.

Elastic considerations

Let us start by building a minimal model of membrane asymmetry that acknowledges compositional asymmetry and includes the resulting elastic ramifications in a series of refinements [12]. In what follows, we will broadly consider two 'kinds' of leaflet asymmetry: composition asymmetry and packing asymmetry; these are illustrated schematically in Figure 1.

We construct a bilayer out of two (at least initially) on-average homogeneous lipid monolayers, whose properties are determined by the number and species of lipid(s) present. The number of lipids in the leaflet is taken to be fixed (though this assumption will be relaxed when considering cholesterol, which more readily flip-flops between the two leaflets, in the 'Cholesterol' section); that is, the leaflet is *not* in contact with any reservoir with which it can exchange lipid molecules. The reference configuration is that of the monolayer found in a flat, tensionless, symmetric membrane, and we will consider small deformations of area and curvature away from this state. To describe a monolayer in this fashion is to consider it as a two-dimensional surface, and as such we must choose a reference surface that represents a molecular aggregate via some idealized geometry, suitable for subsequent theoretical modeling. As it turns out, there exists a unique choice for the reference surface which results in curvature and area deformations contributing to the free energy independently, with no curvature–area cross-coupling; it is called the *neutral surface* [23, 24]. With this choice, our subsequent elastic modeling can consider bending and stretching separately.

If the two leaflets differ in lipid type, they almost surely will also differ in their monolayer bending rigidities $(\kappa_{m+}, \kappa_{m-})$ and spontaneous curvatures (K_{m+}, K_{m-}) . To be clear about the sign of geometric quantities such as the mean curvature, we will assume that bilayer quantities will follow the same sign convention as the upper ('+') leaflet.

As long as the two leaflets can slide past one another, their curvature elastic surface energy densities — in classical Helfrich fashion [25] — can be written as separate bending terms for each one:

$$e_0(K) = \frac{1}{2} \kappa_{m+} (K_+ - K_{m+})^2 + \frac{1}{2} \kappa_{m-} (K_- + K_{m-})^2.$$
 (1)

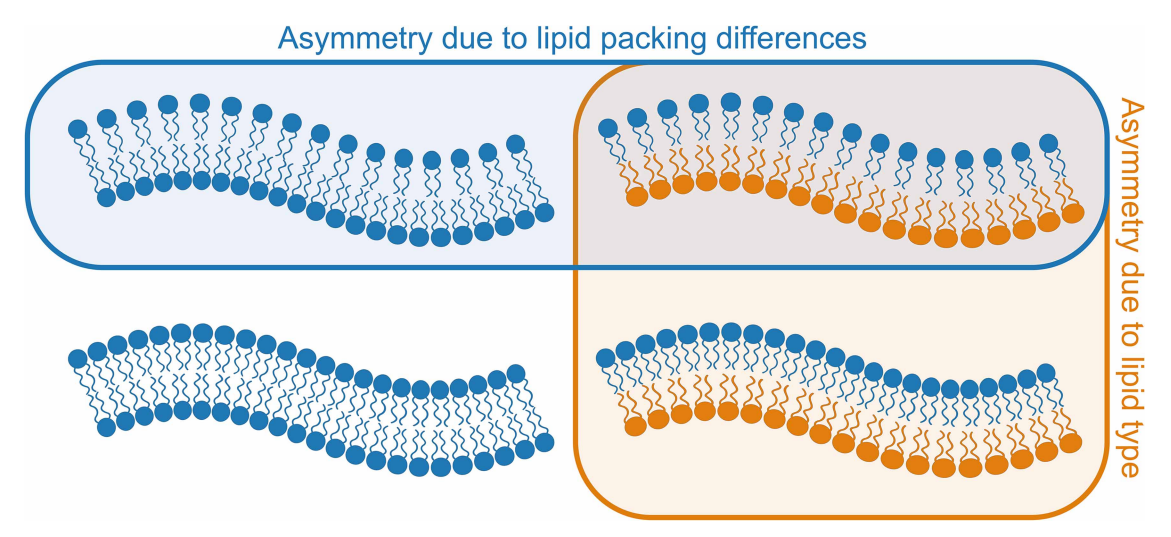


FIG. 1. Different phenomena can contribute to the asymmetric state of lipid membranes.

The common notion of compositional asymmetry refers to the fact that one leaflet contains different lipids, or a different lipid mixture, than the other one (illustrated by differently colored lipids on the right side of the diagram); this generally leads to a nonzero spontaneous bilayer curvature dependent on lipid materials properties. But it is also possible that the two leaflets are differently packed as illustrated in the top row of the diagram, creating a spontaneous curvature more akin to that of bimetallic strips. In general, both effects contribute together and could even cancel (see also Figure 3).



The first/second term captures the upper/lower leaflet, and the +-sign in front of $K_{\rm m-}$ is necessary because the lipids in the lower leaflet are flipped compared with the upper one, but the curvature sign convention stays the same. Observe that we dropped a second quadratic term proportional to the Gaussian curvature $K_{\rm G}$, since we will not be interested in effects arising from edges or topology. More importantly, eqn (1) also drops a constant tension term, meaning we will for now assume that the two leaflets are individually tensionless. Equation (1) is written as depending only on K, the bilayer midsurface curvature, since in a bilayer the two monolayer curvatures cannot truly be independent, as their 'bottom' surfaces coincide. Whatever reference surfaces we use to define K_{\pm} for the monolayers will be parallel to this midsurface (neglecting lipid tilt), offset by some normal displacement z (illustrated in Figure 2), which as stated previously is most conveniently chosen to be the relative displacement of the neutral surface from the midsurface. The curvature of such a parallel surface, $K_{||}(z)$, can be related to the midsurface curvature K by $K_{||}(z) = K + (2K_{\rm G} - K^2)z + \mathcal{O}(z^2)$ [26, 27]. Inserting this expression into eqn (1) yields leading corrections linear in z and higher order in curvature, which we neglect. Therefore in what follows, we relax the distinction between the curvatures of the two monolayers, treating them both as approximately equal to K. The results that follow should therefore be considered small-curvature approximations, though this is already true of the Helfrich functional itself.

Generally, the minimum energy state of an asymmetric membrane as described by eqn (1) is not flat. Instead, the bilayer assumes a preferred curvature given by

$$\frac{\partial e_0(K)}{\partial K}\Big|_{K=K_{0b}} = 0 \implies K_{0b} = \frac{\kappa_{m+}K_{m+} - \kappa_{m-}K_{m-}}{\kappa_{m+} + \kappa_{m-}}.$$
 (2)

This value, K_{0b} , is the rigidity-weighted difference between the individual spontaneous leaflet curvatures and as such a *material parameter*. Interestingly, such a membrane would have a net spontaneous curvature even if $K_{m+} = K_{m-}$, as long as the rigidities $\kappa_m \pm$ differ. The reason is that neither leaflet wants to be flat, but the one with the larger rigidity is less willing to compromise. Observe that we can now write the bilayer energy as

$$e_0(K) = \text{const.} + \frac{1}{2}\kappa(K - K_{0b})^2,$$
 (3)

where $\kappa = \kappa_{\rm m+} + \kappa_{\rm m-}$ is the bilayer bending modulus; the constant may be absorbed in the net bilayer tension. Unlike the curvature difference between the two leaflets, the *area* difference cannot be ignored, since it contributes to important leading-order physics if we wish to consider differential strain and stress. Specifically, the area element $dA_{||}(z)$ of a parallel surface (see again Figure 2) a displacement z away from the bilayer midplane is given by $dA_{||}(z) = dA(1 + Kz + K_G z^2)$ [26, 27]. This expression is actually exact, but we will only need the leading order in z to calculate an area strain for the two curved leaflets, evaluated at the distances z_{\pm} of the

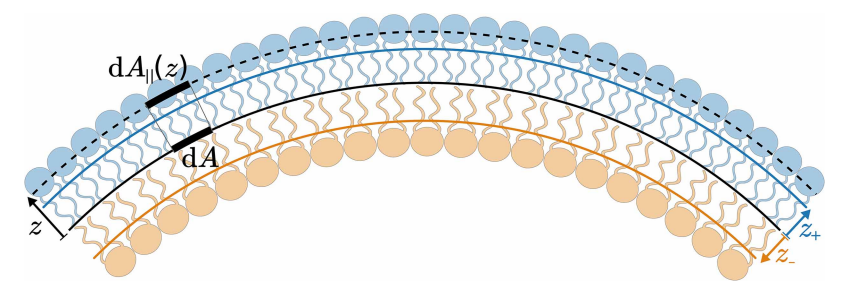


FIG. 2. Illustration of the different quantities involved in membrane elasticity calculations.

The solid black curve indicates the bilayer midsurface. The dashed black curve is a parallel surface a displacement z away from the midsurface. $dA_{||}(z)$ is the area element on the parallel surface, which can be related to dA on the midsurface with knowledge of its curvature, as described in the text. The solid colored lines indicate the monolayer neutral surfaces, at which bending and stretching elastically decouple, a distance z_{\pm} away from the midsurface.



leaflets' respective neutral surfaces:

$$\gamma_{+}(\bar{K}) = \pm (\bar{K} - K_{0s})z_{\pm} + \mathcal{O}(z_{+}^{2}).$$
 (4)

Note that the leaflet strains γ_{\pm} depend on the *surface-averaged* curvature \bar{K} taken over the entire membrane, because the leaflets can slide past each other and the only trans-leaflet area difference that matters is the global one. K_{0s} is the bilayer curvature at which a conceivably existing differential area strain vanishes. This special curvature clearly depends on how the bilayer was made (e.g., if one side was over-packed compared with the other one) and is therefore not a material parameter but rather an 'initial condition'. We also note here that z_{\pm} is considered a monolayer material property, and taken as the *positive* distance from the bilayer midsurface to the monolayer neutral surface. As such, when substituting it into the previously presented expressions for $dA_{||}(z)$ and $K_{||}(z)$, the appropriate sign must be included based on whether the leaflet is above or below the midsurface in the chosen coordinate system.

Writing the monolayer area expansion moduli as $K_{A,m\pm}$, we can equip the leaflets with an additional stretching energy of the form

$$e_{\rm nl} = \frac{1}{2} K_{A,m+} \gamma_+^2(\bar{K}) + \frac{1}{2} K_{A,m-} \gamma_-^2(\bar{K})$$
 (5a)

$$= \frac{1}{2} \kappa_{\rm nl} (\bar{K} - K_{0s})^2, \tag{5b}$$

where

$$\kappa_{\rm nl} := K_{A.m+} z_{\perp}^2 + K_{A.m-} z_{\perp}^2 \stackrel{*}{\approx} K_A z_0^2.$$
(6)

Equation (5b) looks like a bending energy density, but it is *non-local*: it is simply the extensive monolayer strain energy divided by the bilayer area A. For this reason, κ_{nl} is known as a 'non-local bending modulus'. The second step of eqn (6) offers a simple expression for it which additionally assumes that $z_+ = z_- \equiv z_0$ and also defines the bilayer area expansion modulus $K_A = K_{A,m-} + K_{A,m-}$. Plugging in typical numbers it is easy to see that κ_{nl} is about 6 times larger than κ , which is one way to quantify the notion that membranes are easier to bend than to stretch that circumvents the issue that κ and K_A really have different dimensions.

Non-local bending models such as these have indeed been proposed in the past [28–33], but they have typically been viewed as *alternatives* to the local Helfrich energy, not as an *addition*. Taking the second view, the total bilayer energy is of the form

$$E_{
m tot} = \int\limits_{\mathcal{M}} rac{1}{2} \kappa (K - K_{0
m b})^2 \, \mathrm{d}A + rac{1}{2} \kappa_{
m nl} \Biggl(rac{1}{A} \int\limits_{\mathcal{M}} K \, \mathrm{d}A - K_{0
m s}\Biggr)^2 \cdot A,$$

or, expressed as an energy density,

$$e_{\text{tot}}(K,\bar{K}) = \frac{1}{2}\kappa(K - K_{0b})^2 + \frac{1}{2}\kappa_{\text{nl}}(\bar{K} - K_{0s})^2, \tag{7}$$

which consist of two terms — a local one that quadratically penalizes bending away from a materials-dependent curvature K_{0b} , and a non-local one that quadratically penalizes average bending away from a curvature strain K_{0s} that is a measure of an initially imposed area strain. Here we must again caution the reader than the second term in eqn (7) is not a *local* energy density depending on the local curvature K, but rather an average energy per unit area depending on the surface-averaged curvature \bar{K} . It is only properly meaningful when this expression is integrated over the entire membrane, which for the second term amounts to multiplication by K. However, if we restrict to constant mean curvature surfaces (in particular: planes, spheres, and cylinders), for which K = K, we can again ask — just as we did in eqn (2) — at what specific curvature this energy



is minimized. This leads to

$$\left. \frac{\partial e_{\text{tot}}(K,K)}{\partial K} \right|_{K=K_0^*} = 0 \implies K_0^* = \frac{\kappa K_{0b} + \kappa_{\text{nl}} K_{0s}}{\kappa + \kappa_{\text{nl}}}.$$
 (8)

The resulting spontaneous curvature is a weighted average between the two characteristic spontaneous curvatures we have encountered now, K_{0b} and K_{0s} , and as such balances between materials properties and initial conditions. This quantifies the notion that lipid curvature and lipid packing are two complementary ways for a membrane to be asymmetric, and that in general both effects contribute to a membrane's overall curvature elastic behavior — see Figure 3.

It is crucial to realize that the curvature energy minimized state at $K = K_0^*$ still exhibits nonvanishing leaflet strains γ_{\pm} (because generally $K_0^* \neq K_{0s}$) and as such different tensions in the two leaflets:

$$\gamma_{\pm} = \pm (K_0^* - K_{0s}) z_{\pm} \Longrightarrow \Sigma_{\pm} = K_{A,m\pm} \gamma_{\pm} \approx \pm \frac{\kappa}{2z_0} \frac{K_{0b} - K_{0s}}{1 + \kappa/\kappa_{nl}}. \tag{9}$$

We find it convenient to define the collective symmetrized and anti-symmetrized versions of these tensions as

$$\begin{array}{ll} \text{net tension:} & \Sigma = \Sigma_{+} + \Sigma_{-} \\ \text{differential stress:} & \Delta \Sigma = \Sigma_{+} - \Sigma_{-} \end{array} \right\} \longleftrightarrow \begin{cases} \Sigma_{+} = \frac{1}{2} (\Sigma + \Delta \Sigma) \\ \Sigma_{-} = \frac{1}{2} (\Sigma - \Delta \Sigma) \end{cases}, \tag{10}$$

because often $\Sigma = 0$ and then one of the two collective variables becomes 'trivial'.

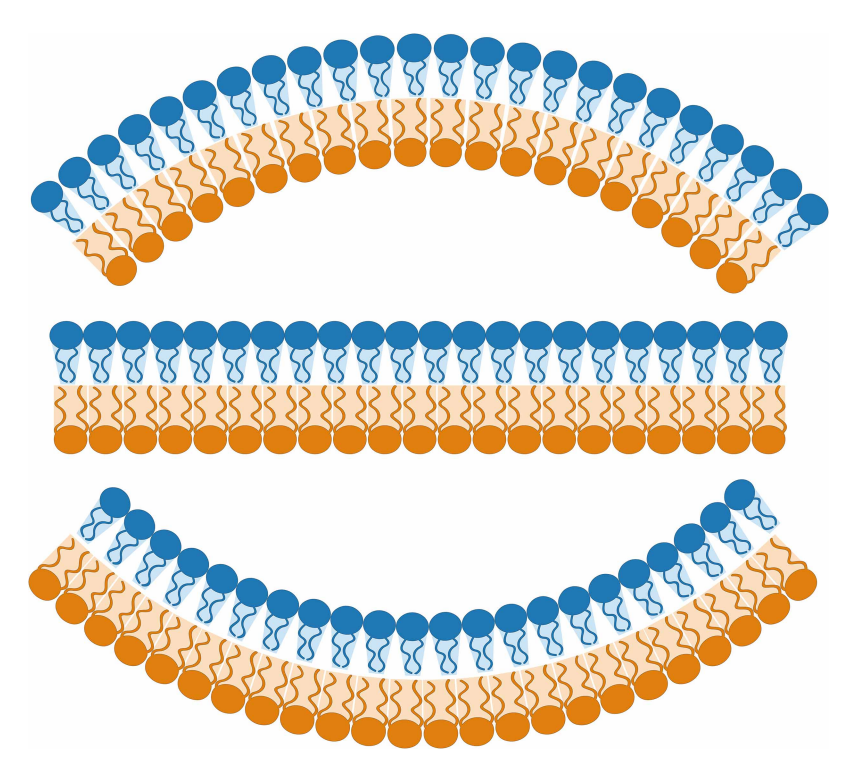


FIG. 3. Illustration of different possible curvature outcomes for an asymmetric bilayer.

The upper leaflet lipids (blue) have a positive spontaneous materials curvature $K_{0b} > 0$, whereas the lower leaflet lipids (orange) have $K_{0b} \approx 0$. However, by suitably over-packing the lower leaflet (creating a $K_{0s} < 0$), any of the three possibilities shown could be realized through a trade-off between area and curvature relaxation, as encapsulated in eqn (8). The case of a flat bilayer is achieved when these two torques balance one another, leaving a residual differential stress given by eqn (11).



The fact that a materials curvature can beat against an imposed initial condition means that we can imagine compositionally asymmetric membranes which are nevertheless geometrically flat, as illustrated in Figure 3. The price to pay is that these systems are differentially stressed. For a spontaneously flat system, $K_0^* = 0$, eqn (8) implies $K_{0s} = -(\kappa/\kappa_{nl})K_{0b}$, and therefore eqns (9) and (10) give

$$\Delta\Sigma(K_0^* = 0) = \frac{\kappa K_{0b}}{z_0}.\tag{11}$$

This condition can also be seen as a *torque balance*: the usual pure-bending torque of a bilayer described by the energy from eqn (3) is $\mathcal{T}_b = \partial \epsilon_0(K)/\partial K = \kappa(K-K_{0b})$, which gives $-\kappa K_{0b}$ for a flat membrane. The stress derived torque is the tension multiplied by the lever arm at which it is acting, giving $\mathcal{T}_s = \Sigma_+ z_+ - \Sigma_- z_- \approx \Delta \Sigma z_0$, which shows that eqn (11) is equivalent to $\mathcal{T}_b + \mathcal{T}_s = 0$.

We often consider the special case of zero bilayer tension, despite this seldom being the case in living membranes [34]. One reason for this is the mathematical simplification afforded by this assumption; however, another reason is that cellular membrane tensions are often negligible compared with the substantial magnitude of differential tensions which must arise in fairly ordinary asymmetric membranes. Consider for instance an asymmetric membrane consisting of DOPC and POPC (as used in the experiments of Elani *et al.* [35]): the former has a spontaneous leaflet curvature of about $K_{\rm m}\approx -0.071\,{\rm nm}^{-1}$, while the latter has $K_{\rm m}\approx -0.032\,{\rm nm}^{-1}$ [36]. Their bending rigidities are almost the same, giving such a DOPC/POPC bilayer a spontaneous materials curvature of $K_{0\rm b}\approx -0.02\,{\rm nm}^{-1}$. Using typical values $z_0\approx 1\,{\rm nm}$ and $\kappa\approx 30\,k_{\rm B}T$ [36], eqn (11) yields $\Delta\Sigma\approx 2.5\,{\rm mN/m}$. This is about two orders of magnitude larger than common net bilayer tensions arising in cells [34] and not too far off bilayer rupture tension [37]. Such large mechanical stresses should at some point impact bilayer integrity, and a recent (coarse-grained) simulation study has indeed shown that the compressed leaflet can reduce its packing stress by ejecting lipids into the tense leaflet (via strongly enhanced directional flip-flop) or alternatively into the aqueous phase (in the form of micellar buds) [38].

One reason why we should expect such tensions to arise in real systems is simply that we can make giant unilamellar vesicles (GUVs) with this type of spontaneous materials curvature asymmetry. Recall that the value of $K_{0b} \approx -0.02\,\mathrm{nm}^{-1}$ for the GUVs in [35] corresponds to a (spherical) curvature radius of $R=2/|K_{0b}|\approx 100\,\mathrm{nm}$. This is *much* smaller than the size of such GUVs, and we would expect them to immediately succumb to the enormous curvature torques by tubulating. The fact that they do not suggest that a counter-torque — conceivably due to differential stress — stabilizes them.

Throughout this section, we have tacitly assumed that elastic parameters such as κ and K_A are insensitive to imposed asymmetry and its associated area strains. While in reality these 'constants' are not constant and vary with quantities such as temperature, pressure, strain, etc., these variations tend to be small in magnitude compared with the value of the parameters themselves (see, e.g. Figure 3d of [12]). However, for systems already near a phase transition, one may rightfully worry that significant differential stresses could lead to radical changes in membrane elastic properties by driving one half of the composite system through a phase transition. This has indeed been observed in simulation [12, 13], and requires more careful thought about the coupling of asymmetry and first-order phase transitions, which we explore in the next section.

Coupling of asymmetry to phase behavior

Even though the differential stress in a membrane can be large, it is not at all obvious how we would measure it. Classical techniques such as flicker spectroscopy [39] or micropipette aspiration [40] are only sensitive to the net tension Σ , not the differential stress $\Delta\Sigma$. Recently developed tension sensitive fluorescent probes [41–43] could be a way forward, if one can modify them such that they remain localized in a single leaflet. Unfortunately these probes respond most immediately to (tension dependent) lipid *packing*, which raises the challenge of disentangling tension from a potentially nontrivial lipid phase behavior (such as, most importantly, an l_o/l_d phase coexistence [44–46]). But then, if tension is correlated to phase behavior, maybe the latter can all by itself act as a tension sensor?

With this in mind, it is instructive to examine how differential stress affects the main phase transition of a bilayer — the transition between a fluid phase and a more tightly packed and elastically more rigid gel phase [47]. The key difference in theoretically describing this scenario is that the free energy is not merely a quadratic function of strain, as in eqn (5a), but a more complicated expression that has a double minimum accounting



for the two different phases. For simplicity, only the case of a single-component membrane is considered, such that the only possible asymmetry to impose is in the number of lipids N_{\pm} populating each leaflet, taken as fixed on the time scale of interest. We will also assume that the membrane remains flat, such that the two leaflets occupy identical area A. Although this is obviously not the most general case, it serves as a simplified starting point from which we can learn the basic impact of differential stress on phase transitions. Modifications to the differential stress originating from curvature stresses can be added into the free energy to generate a more robust theory; however, we are not aware of any work which has yet included this level of detail.

Let us take a to be specific lipid area and assume that the function $f_m(a)$ is the specific free energy of one monolayer at the phase transition temperature under zero tension (and hence its two free energy minima have the same height). Applying a monolayer tension σ_T will then shift the relative height of these minima, giving us

$$f_{\rm m}(a,\sigma_T) = \bar{f}_{\rm m}(a) - \sigma_T a. \tag{12}$$

Although σ_T evidently contributes to the monolayer tension, for the present purpose our viewpoint is that $f_{\rm m}(a,\sigma_T)$ is the Helmholtz free energy and σ_T is simply an intensive parameter which de-tunes the minima such that they no longer have the same free energy. In particular, σ_T can be re-interpreted as a temperature increment proportional to $(T-T_{\rm gel})/T_{\rm gel}$ by utilizing the Clausius–Clapeyron equation [47]. The primary motivation for this is to act as a stand-in for the temperature dependence of the free energy, the form of which is not known *a priori*. As such, in what follows, σ_T is best regarded as a tension-valued stand-in for a temperature (hence the subscript T) increment away from the main phase transition temperature, and we emphasize that it is *not* the variable representing the present tension in either the monolayer or bilayer.

Especially when analyzing simulations of differentially stressed systems near their main phase transition, it is important to account for finite size corrections that arise when part of a leaflet goes into a gel phase, creating non-extensive line tension contributions to the free energy. In such small simulations, these non-extensive terms must be taken into account through a leaflet free energy determined by

$$F_{\rm m}(a,N;\sigma_T) = \min \left\{ \frac{N f_{\rm m}(a,\sigma_T)}{N f_{\rm m}^*(a,\sigma_T) + \Delta F_{\gamma}} \right\},\tag{13}$$

where N is the number of lipids in the monolayer, a is the area per lipid in the particular monolayer, $f_{\rm m}^*(a,\sigma_T)$ is the convex envelope of $f_{\rm m}(a,\sigma_T)$, and ΔF_{γ} is any type of line tension term that could arise, such as the boundary of a circular domain or a stripe extending across the periodic boundary conditions. Neglecting contributions due to inter-leaflet coupling, the free energy for a flat bilayer with area A is the sum of two such expressions, each evaluated at the corresponding asymmetry-dependent monolayer area per lipid,

$$F(A, N_0; \delta n, \sigma_T) = \underbrace{F_{\text{m}}\left(\frac{A}{N_0(1+\delta n)}, N_0(1+\delta n); \sigma_T\right)}_{F_{\text{max}}} + \underbrace{F_{\text{m}}\left(\frac{A}{N_0(1-\delta n)}, N_0(1-\delta n); \sigma_T\right)}_{F_{\text{max}}}, \tag{14}$$

where $\delta n = (N_+ - N_-)/(N_+ + N_-)$ is the relative lipid packing asymmetry between the two leaflets and $N_0 = (N_+ + N_-)/2$ is their average lipid number. As before, + and - refer to the upper and lower monolayers, respectively, such that $\delta n > 0$ corresponds to the + leaflet containing a larger number of lipids.

At vanishing bilayer tension, $\Sigma \equiv \partial F/\partial A = 0$, the membrane takes on the area $A_{\rm eq}$ which minimizes eqn (14). The presence of fluid–gel coexistence in either leaflet can then be determined by checking whether $A_{\rm eq}$ lies within the coexistence region of each individual monolayer free energy $F_{\rm m\pm}$, and the fractional gel content of the leaflet is determined by how far along the double-tangent this area is (the lever rule). This is illustrated in Figure 4a in the thermodynamic limit, in which case the coexistence region for each monolayer coincides with its double-tangent construction. Importantly, note how the corresponding monolayer free energies have slopes which are negatives of each other at the equilibrium area, displaying the cancellation of equal but opposite monolayer tensions (differential stress) which give rise to the net tensionless bilayer. By following this procedure for a range of values of δn and σ_T , one constructs a phase coexistence diagram for the bilayer like the



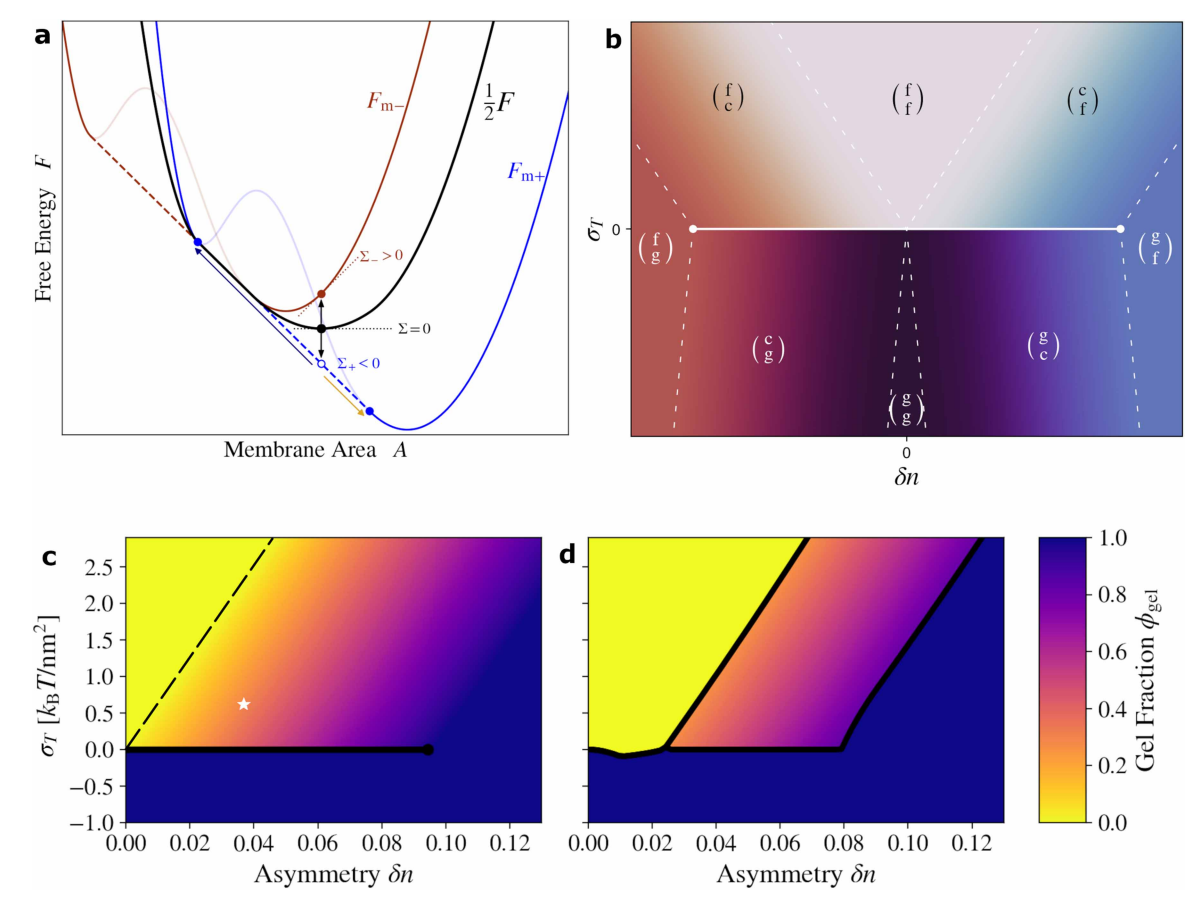


FIG. 4. (a) Helmholtz free energy as a function of membrane area A for δn and σ_T corresponding to the star in **c**. The monolayer free energies (brown and blue curves) are labeled as $F_{m\pm}$ (as shown in eqn (14)). The black curve is one half of their sum. The indicated point on F gives the zero tension state (hence the horizontal tangent), and the corresponding monolayer points and their slopes are indicated. The corresponding point on F_{m+} (blue open circle) lies within this monolayer's coexistence region (dashed double-tangent construction) and therefore this leaflet exhibits phase separation to the points at either end of the double-tangent (blue solid points). (b) Complete qualitative phase diagram for a tensionless bilayer as predicted by eqn (14), labeling the 8 different phase regions. In each label, the upper/lower letter describes the state of the +/leaflet, respectively. The letter 'f' corresponds to fluid, 'g' to gel, and 'c' to coexisting fluid and gel. For example, the label $\begin{pmatrix} c \\ g \end{pmatrix}$ means that the + leaflet has coexisting fluid and gel while the - leaflet is entirely gel. Dashed white lines indicate boundaries between these regions across which there is no discontinuous change in gel/fluid fraction. The solid white line indicates the boundary across which discontinuous transitions occur. (c) Phase coexistence diagram calculated from eqn 14 for the + leaflet of a net tensionless bilayer in the thermodynamic limit, using parameters inferred from Martini DLPC simulations [47]. Yellow indicates fluid, blue indicates gel, and colors in between correspond to intermediate compositions (coexistence). The dashed line indicates the boundary between fluid and coexistence. (d) Phase coexistence diagram for the same system as (c), but for a periodic rectangular system of finite size with shortest side-length 8 nm. The solid lines indicate boundaries of discontinuous transitions.

one shown in Figure 4b. This figure labels all of the qualitatively different phase regions that are possible for the system. As stated before, $\delta n > 0$ corresponds to the + leaflet having more lipids than the - leaflet, and vice-versa for $\delta n < 0$. As such, the left half of Figure 4b is essentially a 'mirror image' of the right half, where the + and - leaflets have exchanged their roles. As such it is sufficient to restrict our analysis to $\delta n > 0$ (this is not true in the general case where there are different lipid species on either side of the bilayer; in that case the two signs of δn do not simply correspond to mirroring the bilayer across its midplane). Examining one monolayer individually leads to a plot such as Figure 4c. Figure 4d is an example of a phase coexistence diagram for a finite system in which non-extensive contributions to the free energy give rise to new



discontinuous transitions not present in the thermodynamic limit. In either case, upon cooling a fluid membrane with $\delta n > 0$, the ordinary fluid to gel phase transition is preceded by the appearance of stable gel domains within the otherwise fluid + leaflet. For details of the simulations from which the parameters for Figure 4c,d are inferred, the reader is referred to Foley *et al.* [47]. This process can just as well be carried out in reverse, yielding a recipe for determining δn by measuring the gel fraction of a leaflet.

If one's goal is to deduce differential stress from phase coexistence, then the boundary between the all-fluid and coexistence regions of the phase diagram is of particular interest. In the thermodynamic limit, one can show that the temperature of the upper phase coexistence boundary (dashed line in Figure 4c) is approximately [47]

$$T_{\rm pc} \approx T_{\rm gel} \left(1 + \frac{\Delta \Sigma \Delta a}{2\Delta q_{\rm m}} \right),$$
 (15)

where Δa is the difference in area per lipid between the fluid and gel phases, $\Delta q_{\rm m}$ is the monolayer specific latent heat, and $\Delta \Sigma$ is the differential stress. Although the slope of this boundary appears to remain roughly the same even for systems of finite size (Figure 4d), the precise location of the boundary in this case depends strongly on the shape of the non-convex portion of the homogeneous free energy, which makes writing an analytical approximation much more difficult.

Taking eqn (15) at face value allows us to calculate some reasonable estimates of how large these effects can be. For the DPPC fluid to ripple transition, by plugging in some experimentally measured values one can show that $T_{\rm pc}-T_{\rm gel}$ increases by about half a degree for each mN/m of differential stress [47–50]. Extrapolating the same ideas to the potentially more interesting case of $l_{\rm o}/l_{\rm d}$ coexistence, the comparatively smaller latent heat of the transition [51, 52] results in the temperature shift being almost an order of magnitude larger for the same differential stress. Thus, not only does phase coexistence appear to be a potential proxy for determining the differential stress state, but differential stress could indeed be a vital 'control dial' which the cell tunes to alter its membranes' phase composition without changing the net tension. Note, however, that more quantitative results for $l_{\rm o}/l_{\rm d}$ phase coexistence would require the construction of a more complex free energy than was used here in order to account for composition dependence, as presented in, e.g. Williamson et al. [53], Wagner et al. [54], or Putzel et al. [55]

Cholesterol

The notion of membrane asymmetry typically requires that lipids stay within their respective leaflet, for otherwise a compositional or packing asymmetry will dissipate over time. This holds for phospholipids, whose characteristic transition ('flip-flop') times between leaflets are measured in hours or days [56, 57], slow enough for active cellular processes to counterbalance a decay in asymmetry. There is an important exception, though: sterols. These small molecules (e.g., cholesterol in animal cells, ergosterol in fungi and protozoa [58]) constitute a significant fraction of cellular membranes (about 30% of the plasma membrane), but their flip-flop times are believed to be in the microsecond range [59–62]. This is too fast for active cellular machinery to keep up, and hence sterols go where thermodynamics drives them, not where we initially put them.

Given this state of affairs, does the notion of differential stress in biomembranes even make sense? If one of the membrane leaflets is compressed while the other one exhibits a sizable tension, and if the membrane also contains a fast-flipping sterol species, would these sterols preferentially redistribute into the tense leaflet and thereby lower the tension? In fact, with sufficiently much sterol available, would it be possible to get the elastic energy associated with differential stress to zero?

That cholesterol can be driven into the tense leaflet has indeed been demonstrated in recent simulations [22, 63]. Moreover, quick back-of-the-envelope calculations show that fairly little cholesterol suffices to cancel rather sizable stresses. Nevertheless, we should not expect cholesterol to do this under all circumstances because other drivers exist that also affect cholesterol. Like in any thermodynamic situation where a given species can freely partition between multiple compartments or phases, the condition that sets its equilibrium distribution is that of equal chemical potential. In our case, differential stress is one of the contributing factors to cholesterol's local chemical potential, but others exist as well. Most notably, entropy strives to even out the cholesterol concentration between the leaflets, and if the lipidome differs between the two sides, cholesterol's free energy of solvation might be different.



To predict how this pans out, we need the free energy of such a system. Unfortunately, this is quite a difficult problem, because cholesterol's mixing behavior with lipids is notoriously subtle. But to get a sense of how a subset of effects balance out, let us examine a simple mean-field solution model that combines linear elasticity for the two leaflets with Flory–Huggins type nonideal mixing [14]. The associated bilayer free energy is then

$$F = \frac{1}{2}K_{A,m+} \frac{(A - A_{+})^{2}}{A_{+}} + \frac{1}{2}K_{A,m-} \frac{(A - A_{-})^{2}}{A_{-}} + k_{B}T \left\{ L_{+} \log \phi_{\ell+} + C_{+} \log \phi_{+} + \chi_{+}L_{+}C_{+} \frac{\sqrt{a_{+}a}}{L_{+}a_{+} + C_{+}a} \right\}$$

$$L_{-} \log \phi_{\ell-} + C_{-} \log \phi_{-} + \chi_{-}L_{-}C_{-} \frac{\sqrt{a_{-}a}}{L_{-}a_{-} + C_{-}a} \right\}. \tag{16}$$

Here, the first line is essentially the elastic stress we have already encountered in eqn (5a), but the equilibrium areas are $A_{\pm} = L_{\pm} a_{\pm} + C_{\pm} a$, where L_{\pm} is the number of phospholipids in the \pm -leaflet, each having area a_{\pm} , while C_{\pm} is the number of cholesterols with area a. Observe that we explicitly assume area additivity, which is not entirely correct in view of cholesterol's ability to condense lipid phases. The second and third line are classical Flory-Huggins expressions for nonideal mixing [64], where the area fractions for phospholipids and cholesterol are defined as

$$\phi_{\ell\pm} = \frac{L_{\pm}a_{\pm}}{L_{+}a_{+} + C_{+}a} \quad \text{and} \quad \phi_{\pm} = \frac{C_{\pm}a}{L_{+}a_{+} + C_{+}a} = 1 - \phi_{\ell\pm}, \tag{17}$$

and χ_{\pm} are the Flory–Huggins χ -parameters that quantify the extent to which cholesterol and phospholipids in each leaflet mix nonideally. (Positive values ultimately lead to phase separation, while negative values mean that the two species prefer to mix.) This free energy needs to be supplemented by two equilibration conditions,

$$\frac{\partial F}{\partial A} = \Sigma = 0$$
 and $\frac{\partial F}{\partial C_{\perp}} = \frac{\partial F}{\partial C_{\perp}}$. (18)

The first defines the external bilayer tension Σ and, for simplicity, sets it to zero; the second equilibrates cholesterol's chemical potential $\mu_{\pm}=\partial F/\partial C_{\pm}$ between the leaflets. It is equivalent to the condition that F is stationary with respect to a change in cholesterol number between the leaflets: $\partial F/\partial (C_{+}-C_{-})=0$.

If we ignore the k_BT -dependent solvation terms in lines 2 and 3 of eqn (16) and only account for elasticity, the condition $\Sigma = 0$ implies for the equilibrium area $A_{\rm eq}$

$$A_{\text{eq}} = \frac{K_{A,\text{m+}} + K_{A,\text{m-}}}{K_{A,\text{m+}}/A_{+} + K_{A,\text{m-}}/A_{-}} \Longrightarrow \begin{cases} F(A_{\text{eq}}) = \frac{1}{2} \frac{(A_{+} - A_{-})^{2}}{A_{+}/K_{A,\text{m+}} + A_{-}/K_{A,\text{m-}}} \\ \Delta \Sigma(A_{\text{eq}}) = -2 \frac{\partial F(A_{\text{eq}})}{\partial (A_{+} - A_{-})} = \frac{2(A_{-} - A_{+})}{A_{+}/K_{A,\text{m+}} + A_{-}/K_{A,\text{m-}}}, \end{cases}$$
(19)

showing that A_{eq} is the $K_{A,\text{m}\pm}$ -weighted harmonic mean between A_+ and A_- , and that the equilibrium free energy is proportional to $(A_+ - A_-)^2$. Observe that both the free energy and the differential stress then vanishes when $A_+ = A_-$, which happens when $C_+ - C_- = (L_- a_- - L_+ a_+)/a$. This shows that if cholesterol indeed were to respond only to elastic drivers, it would distribute such as to eliminate the differential stress.

In general, the differential stress does not vanish, though, and cholesterol does not even out the total areas. Unfortunately, the mixing terms, and especially the fact that all specific lipid areas $\{a_+, a_-, a\}$ are unequal, turns the equilibrium conditions into algebraically unwieldy expressions. However, we can get a good qualitative idea for how the system behaves if we, first, make the (pretty rough) equal area ('e.a.') approximation $a_+ = a_- = a$, and second, expand the resulting equilibrium conditions for small deviations from the symmetric state — meaning we assume that the membrane is only weakly asymmetric, in terms of both packing and solvation driving forces. If we define the relative lipid and cholesterol asymmetries $\{\delta\ell, \delta c\}$ and the cholesterol mol



fraction ϕ via

$$\delta \ell := \frac{L_{+} - L_{-}}{L_{+} + L_{-}}, \quad \delta c := \frac{C_{+} - C_{-}}{C_{+} + C_{-}} \quad \text{and} \quad \phi := \frac{C}{L_{+} + L_{-} + C}$$
 (20)

and also assume that the χ -parameter vanishes on average, such that $\chi_{\pm}=\pm\frac{1}{2}\delta\chi$, then we can show that [14]

$$2 \, \delta c(\delta \chi, \delta \ell) \stackrel{\text{e.a.}}{\approx} - \frac{(1 - \phi)^2 \delta \chi + (\tilde{K}_A - 2)(1 - \phi) \delta \ell}{1 + \frac{1}{2} (\tilde{K}_A - 2) \phi}, \tag{21a}$$

$$2 \, \delta c(\delta \chi, \Delta \tilde{\Sigma}_0) \stackrel{\text{e.a.}}{\approx} (\tilde{K}_A - 2) \Delta \tilde{\Sigma}_0 - (1 - \phi)^2 \delta \chi, \tag{21b}$$

where $\tilde{K}_A = K_A a/k_B T$ and $\Delta \tilde{\Sigma} = \Delta \Sigma/K_A$ are a suitably scaled elastic stretching modulus and differential stress, respectively. What eqns (21a) and (21b) show is that cholesterol asymmetry, lipid asymmetry, partitioning preference, and differential stress are all connected by simple linear relations that only depend on the membrane's lateral stretching modulus and the cholesterol mol fraction. This is encouraging, because neither δc nor $\delta \Sigma$ are currently among the observables we know how to experimentally measure. The linear dependencies suggest that differential stress does not enter as yet another 'hidden variable' into the already complicated asymmetric membrane thermodynamics, but that thermodynamic models such as eqn (16) strongly constrain it. Of course, more refined models would likely predict correspondingly more complicated dependencies, but it seems advantageous that such constraints must exist in the first place.

Let us illustrate this theoretical model using one specific example, the human red blood cell. Its leaflet-resolved lipidome is extremely well characterized [7], with the notable exception of cholesterol, which accounts for 40 mol% of the total lipid content but whose leaflet distribution is unknown. This system is particularly interesting since recent experiments suggest that the cytosolic (inner) leaflet may contain between 1.7 and 2 times as many phospholipids as the exoplasmic (outer) one [65, 66]. If so, this would suggest that a large amount of cholesterol must be pushed to the outer side to compensate for the large area imbalance. What would the theory resting on eqn (16) say?

To make numerical predictions, let us assume an average cholesterol fraction of $\phi = 40 \text{ mol}\%$ [7] and an area expansion modulus of $K_A = 240 \text{ mN/m}$, which is fairly robust for many lipid membranes [50] but may be an under-estimate considering the large cholesterol content. For the specific lipid areas we take $a_{\text{cyto}} = 0.7 \text{ nm}^2$ and $a_{\text{exo}} = 0.65 \text{ nm}^2$, which accounts for the higher order of the outer leaflet. Given that lipid areas do not simply add in the presence of cholesterol, its area is on shaky ground, but we shall use $a = 0.35 \text{ nm}^2$ in view of its effective area in Chol–DPPC mixtures [67].

Figure 5 shows the predicted differential stress (upper panel Figure 5a) and the associated cholesterol asymmetry (lower panel Figure 5b) as a function of the partitioning preference of cholesterol — using the full theory associated with eqn (16), not merely the simplified equal-area approximations (eqns 21a and 21b). We show the range $\delta\chi\in[-3,2]$ to give an idea how much a typical solvation bias can shift stresses and the cholesterol distribution (note that $\delta\chi$ is approximately the specific free energy difference per cholesterol in units of k_BT). The vertical blue gradient band around $\delta\chi\approx-2$ indicates a plausible range — based on work by Tsamaloukas et al. [68], who showed that transferring cholesterol from a pure POPC membrane into a membrane in which 50% of lipids have been replaced by sphingomyelin lowers its chemical potential somewhere between $1\,k_BT$ and $3\,k_BT$, depending on the overall cholesterol concentration. The lines correspond to different packing imbalances $\delta\ell$, all the way from $\delta\ell=0$ (black line, no imbalance) to $\delta\ell=-0.35$ (orange line, $L_{\rm cyto}/L_{\rm exo}\approx2$). The experimentally claimed range of phospholipid imbalances lies within $\delta\ell=[-0.25, -0.35]$ and is indicated by the orange band between the three uppermost lines.

Increasing the cytoplasmic abundance of phospholipids increases the differential stress and the percentage of cholesterol in the exoplasmic leaflet. Nevertheless, without any additional driving forces (i.e. at $\delta\chi=0$), the differential stress would still be extremely large: between 15 and 20 mN/m, an effect solely attributable to entropy. Since however the exoplasmic leaflet consists of more ordered lipids, an additional partitioning bias helps translocate even more cholesterol into the outer leaflet and further reduces the differential stress, plausibly to values $\sim\!\!10$ mN/m. As a consequence of these packing and solvation biases, more than $\sim\!\!90\%$ of all cholesterol can be



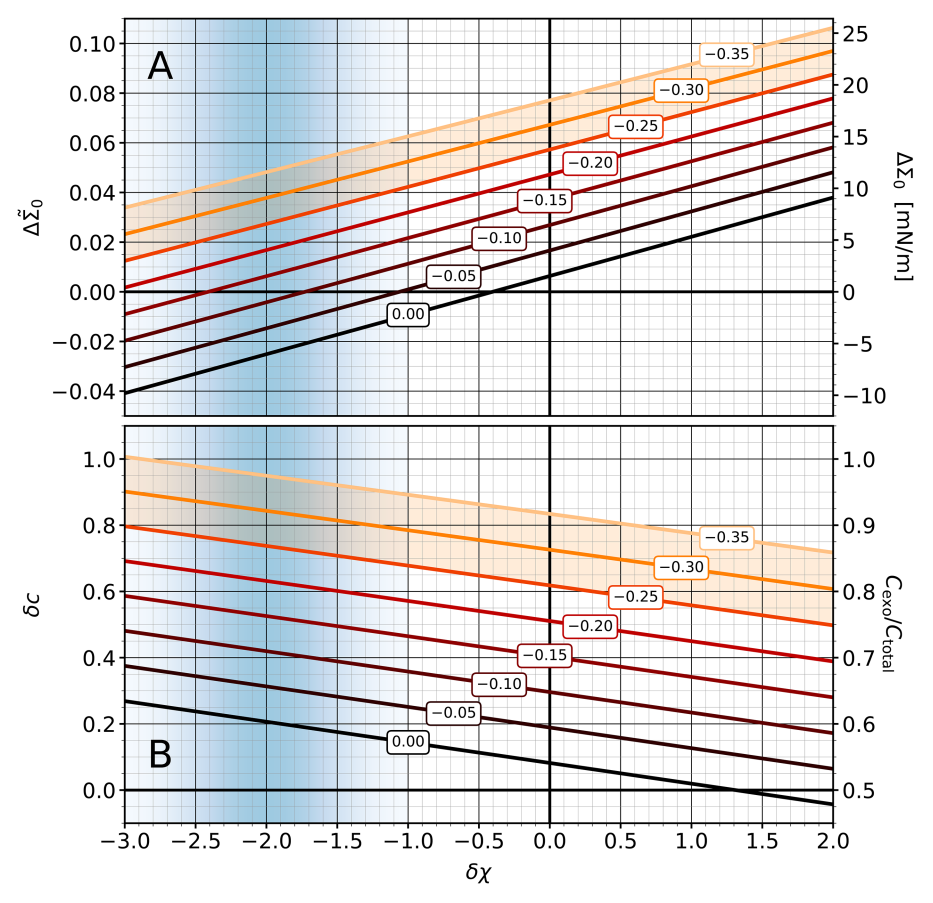


FIG. 5. Differential stress (upper panel (a); left axis: scaled dimensionless version, right axis: SI units) and cholesterol asymmetry (lower panel (b); left axis: scaled asymmetry, right axis: fraction of cholesterol in outer leaflet) as a function of partitioning preference $\delta\chi$. The blue vertical gradient bar centered around $\delta\chi=-2$ gives our best estimate for the partitioning bias in a red blood cell. The black-to-orange lines correspond to a set of phospholipid imbalances $\delta\ell\in\{0,-0.05,-0.1,\ldots,-0.35\}$ as indicated in the boxed labels. The experimental range $L_{\rm cyto}/L_{\rm exo}\in[1.7,2]$ corresponds approximately to $\delta\ell\in[-0.25,-0.35]$ and is indicated by the shaded orange band.

found in the exoplasmic leaflet. Its mol fraction there is given by

$$x_{\text{chol,exo}} = \frac{C_{+}}{L_{+} + C_{+}} = \frac{\phi(1 + \delta c)}{1 + \phi \delta c + (1 - \phi)\delta \ell},$$
 (22)

which can reach somewhere between 60% and 65%, depending on $\delta\ell$. This is getting very close to cholesterol's solubility limit (\sim 66% in bilayers whose lipids have phosphatidylcholine headgroups [69]), indicating that this membrane exhibits several extreme conditions and lies close to the border of an instability. To what extent these predictions are correct depends on how strong the actual phospholipid imbalance in red blood cell membranes actually is, and how reliable the simple theory used for interpreting the data is. Nevertheless, it seems likely that this membrane — and maybe other plasma membranes as well — are less calm and placid than common expectation holds, exhibiting not just sizable phospholipid asymmetries but also cholesterol imbalances (despite its ability to flip-flop) and strong differential stresses, with obvious implications for its equilibrium state of curvature.

Experimental signatures

We have argued that differential stress may be a key elastic player in the mechanics and thermodynamics of lipid membranes. Unfortunately, to this date no experimental method exists that can directly measure it.



However, we have argued that its magnitude can be quite sizable (if compared with other typical tensions arising in the system), and so it should noticeably affect many other observables that are experimentally accessible and can therefore act as 'proxies'. Let us therefore conclude with four observations and speculations that might help anchor differential stress firmly in observable territory.

- 1. Several studies have measured the bending rigidity of compositionally asymmetric vesicles and found it can be larger than the naïvely expected average of the two cognate symmetric membranes: increases between 50% [70, 71] and 150% [35] have been reported. There is no known mechanism by which lipid leaflets become much stiffer due to the mere presence of a different-type leaflet. But it is conceivable that the substantial spontaneous curvature which such asymmetric bilayers possess necessitates a balancing differential stress in order to render GUVs stable in the first place. If so, this stress could affect the rigidity, as compressed leaflets are expected to be stiffer. Using coarse-grained simulations at the Martini level, Hossein and Deserno found this hypothesis viable: significant increases in the curvature elasticity of one-component membranes could be driven by sufficient differential stress [12]. They subsequently found that this rigidity increase might be related to the formation of gel domains in the compressed leaflet [13].
- 2. Given the impact asymmetry has on the gel transition, studying asymmetric vesicles close to that transition should provide multiple interesting signatures. Both the shift of T_{gel} as well as the gel fraction in the compressed phase should be observable either via fluorescent techniques, or through thermodynamic means. Indeed, Eicher et al. [72] have recently studied this transition via differential scanning calorimetry in POPC/POPE LUVs and found that the nature of the transition depended on which lipid species was in the outer layer. Revisiting the asymmetric creation protocol might unveil which side would be put under differential stress and hence how the transition might get affected. However, given the small size of LUVs (diameter O(100 nm)), spontaneous curvature effects will likely also play a role.
- 3. Cholesterol containing vesicles can be bending torque relaxed for two very different reasons: either because cholesterol helps to *lower* differential stress by 'filling in the holes' in a tense leaflet, or because cholesterol actively *creates* a differential stress by pushing into a leaflet consisting of a lipid phase it prefers to solubilize in. If so, then removing cholesterol from such asymmetric vesicles (by exposing it to soluble β -cyclodextrin) would have opposite effects in terms of curvature torque creation, driving the (ideally non-tense) vesicle to either tubulate inwards or outwards, in a way that is in principle predictable from the setup.
- 4. Ion channels are gates for ions through membranes that can be highly selective. For C-type channels this selectivity rests on a narrow filter region that typically extends only through part of the transmembrane path, say, the exoplasmic leaflet [73]. If so, either the gating or the underlying selectivity of these channels should be rather sensitive to differential stress, which could either compress or widen the selectivity filter without any change in the (very low) net bilayer tension. External manipulations of that stress (say, by asymmetric lipid or cholesterol addition/removal via cyclodextrins) should change the channel characteristics and would therefore be electrophysiologically observable. To the best of our knowledge, no simulations of channels testing their sensitivity to differential stress have been conducted, but this would strikes us to be a highly worthwhile endeavor.

Conclusion

Recent progress in artificially creating asymmetric lipid bilayers via multiple preparation protocols [74] has caused a renaissance in the study and understanding of such membranes. The theoretically hypothesized phenomenon of differential stress — presently immeasurable but likely large in magnitude — might significantly impact a large number of elastic and thermodynamic membrane properties and thereby have important functional consequences. The growing interest in studying this phenomenon will help clarify and quantify its physical nature, and how it might contribute to countless membrane associated processes. We hope that some of the theoretical ideas we have reviewed here might offer a guide in this journey.

Summary

• Biomembrane asymmetry extends beyond the lipidome; in particular: the tension in the two individual leaflets can also be different.



- The resulting differential stress affects a wide variety of membrane properties, ranging from geometry over elasticity to thermodynamics.
- Even though sterols can rapidly flip-flop between leaflets, they do not necessarily cancel the differential stress. Their distribution is instead dictated by a balance between elastic stresses, solubility preferences, and entropy.
- While presently not directly measurable, the effect of differential stress on other membrane observables might offer viable ways for assessing it.

Competing Interests

The authors declare that there are no competing interests associated with the manuscript.

Funding

This work was supported, in part, by the National Science Foundation (U.S.A.) via award [NSF/CHE-2102316].

Abbreviations

GUVs, giant unilamellar vesicles.

References

- 1 Alberts, B., Johnson, A., Lewis, J., Raff, M., Roberts, K. and Walter, P. (2002) Molecular Biology of the Cell, Garland Science, New York, NY
- 2 Karp, G. (2009) Cell and Molecular Biology: Concepts and Experiments, John Wiley & Sons, Hoboken, NJ
- 3 Bretscher, M.S. (1972) Asymmetrical lipid bilayer structure for biological membranes. *Nat. New Biol.* **236**, 11–12 https://doi.org/10.1038/newbio/236011a0
- 4 Verkleij, A.J., Zwaal, R.F.A., Roelofsen, B., Comfurius, P., Kastelijn, D. and Van Deenen, L.L.M. (1973) The asymmetric distribution of phospholipids in the human red cell membrane. a combined study using phospholipases and freeze-etch electron microscopy. *Biochim. Biophys. Acta* 323, 178–193 https://doi.org/10.1016/0005-2736(73)90143-0
- Sandra, A. and Pagano, R.E. (1978) Phospholipid asymmetry in LM cell plasma membrane derivatives: polar head group and acyl chain distributions. *Biochemistry* **17**, 332–338 https://doi.org/10.1021/bi00595a022
- 6 Devaux, P.F. (1991) Static and dynamic lipid asymmetry in cell membranes. Biochemistry 30, 1163–1173 https://doi.org/10.1021/bi00219a001
- Toent, J.H., Levental, K.R., Ganesan, L., Rivera-Longsworth, G., Sezgin, E., Doktorova, M. et al. (2020) Plasma membranes are asymmetric in lipid unsaturation, packing and protein shape. *Nat. Chem. Biol.* **16**, 644–652 https://doi.org/10.1038/s41589-020-0529-6
- Traïkia, M., Warschawski, D.E., Lambert, O., Rigaud, J.-L. and Devaux, P.F. (2002) Asymmetrical membranes and surface tension. *Biophys. J.* **83**, 1443–1454 https://doi.org/10.1016/S0006-3495(02)73915-5
- 9 Różycki, B. and Lipowsky, R. (2015) Spontaneous curvature of bilayer membranes from molecular simulations: asymmetric lipid densities and asymmetric adsorption. *J. Chem. Phys.* **142**, 054101 https://doi.org/10.1063/1.4906149
- 10 Marquardt, D., Geier, B. and Pabst, G. (2015) Asymmetric lipid membranes: towards more realistic model systems. Membranes 5, 180–196 https://doi. org/10.3390/membranes5020180
- 11 Weiner, M.D. and Feigenson, G.W. (2019) Molecular dynamics simulations reveal leaflet coupling in compositionally asymmetric phase-separated lipid membranes. J. Phys. Chem. B 123, 3968–3975 https://doi.org/10.1021/acs.jpcb.9b03488
- Hossein, A. and Deserno, M. (2020) Spontaneous curvature, differential stress, and bending modulus of asymmetric lipid membranes. *Biophys. J.* **118**, 624–642 https://doi.org/10.1016/j.bpj.2019.11.3398
- Hossein, A. and Deserno, M. (2021) Stiffening transition in asymmetric lipid bilayers: the role of highly ordered domains and the effect of temperature and size. *J. Chem. Phys.* **154**, 014704 https://doi.org/10.1063/5.0028255
- 14 Varma, M. and Deserno, M. (2022) Distribution of cholesterol in asymmetric membranes driven by composition and differential stress. *Biophys. J.* **121**, 4001–4018 https://doi.org/10.1016/j.bpj.2022.07.032
- 15 Esteban-Martin, S., Risselada, H.J., Salgado, J. and Marrink, S.J. (2009) Stability of asymmetric lipid bilayers assessed by molecular dynamics simulations. *J. Am. Chem. Soc.* **131**, 15194–15202 https://doi.org/10.1021/ja904450t
- 16 Ingólfsson, H.I., Melo, M.N., Van Eerden, F.J., Arnarez, C., Lopez, C.A., Wassenaar, T.A. et al. (2014) Lipid organization of the plasma membrane. J. Am. Chem. Soc. 136, 14554–14559 https://doi.org/10.1021/ja507832e
- Park, S., Beaven, A.H., Klauda, J.B. and Im, W. (2015) How tolerant are membrane simulations with mismatch in area per lipid between leaflets? *J. Chem. Theory Comput.* **11**, 3466–3477 https://doi.org/10.1021/acs.jctc.5b00232
- 18 Sharma, S., Kim, B.N., Stansfeld, P.J., Sansom, M.S.P. and Lindau, M. (2015) A coarse grained model for a lipid membrane with physiological composition and leaflet asymmetry. *PLoS ONE* **10**, e0144814 https://doi.org/10.1371/journal.pone.0144814
- 19 Doktorova, M. and Weinstein, H. (2018) Accurate in silico modeling of asymmetric bilayers based on biophysical principles. *Biophys. J.* 115, 1638–1643 https://doi.org/10.1016/j.bpj.2018.09.008



- 20 Foley, S. and Deserno, M. (2020) Stabilizing leaflet asymmetry under differential stress in a highly coarse-grained lipid membrane model. J. Chem. Theory Comput. 16, 7195–7206 https://doi.org/10.1021/acs.jctc.0c00862
- Park, S., Im, W. and Pastor, R.W. (2021) Developing initial conditions for simulations of asymmetric membranes: a practical recommendation. *Biophys. J.* **120**, 5041–5059 https://doi.org/10.1016/j.bpj.2021.10.009
- 22 Aghaaminiha, M., Farnoud, A.M. and Sharma, S. (2021) Quantitative relationship between cholesterol distribution and ordering of lipids in asymmetric lipid bilayers. *Soft Matter* **17**, 2742–2752 https://doi.org/10.1039/DOSM01709D
- 23 Campelo, F., Arnarez, C., Marrink, S.J. and Kozlov, M.M. (2014) Helfrich model of membrane bending: from Gibbs theory of liquid interfaces to membranes as thick anisotropic elastic layers. Adv. Colloid Interface Sci. 208, 25–33 https://doi.org/10.1016/j.cis.2014.01.018
- 24 Kozlov, M.M. and Winterhalter, M. (1991) Elastic moduli for strongly curved monoplayers. Position of the neutral surface. J. Phys. ll 1, 1077–1084 https://doi.org/10.1051/jp2:1991201
- 425 Helfrich, W. (1973) Elastic properties of lipid bilayers: theory and possible experiments. Z. Naturforsch. C 28, 693–703 https://doi.org/10.1515/znc-1973-11-1209
- 26 Deserno, M. (2015) Fluid lipid membranes: from differential geometry to curvature stresses. Chem. Phys. Lipids 185, 11–45 https://doi.org/10.1016/j.chemphyslip.2014.05.001
- 27 Do Carmo, M.P. (2016) Differential Geometry of Curves and Surfaces: Revised and Updated, 2nd edn, Dover, Mineola, NY
- Evans, E.A. (1974) Bending resistance and chemically induced moments in membrane bilayers. Biophys. J. 14, 923–931 https://doi.org/10.1016/ S0006-3495(74)85959-X
- Evans, E.A. (1980) Minimum energy analysis of membrane deformation applied to pipet aspiration and surface adhesion of red blood cells. *Biophys. J.* **30**, 265–284 https://doi.org/10.1016/S0006-3495(80)85093-4
- 30 Svetina, S., Brumen, M. and Zeks, B. (1985) Lipid bilayer elasticity and the bilayer couple interpretation of red-cell shape transformations and lysis. Stud. Biophys. 110, 177–184
- 31 Seifert, U., Miao, L., Döbereiner, H.-G. and Wortis, M. (1992) Budding transition for bilayer fluid vesicles with area-difference elasticity. In *The Structure* and Conformation of Amphiphilic Membranes (Lipowsky, R., Richter, D. and Kremer, K., eds), pp. 93–96. Springer, Heidelberg, Germany
- Heinrich, V., Svetina, S. and Žekš, B. (1993) Nonaxisymmetric vesicle shapes in a generalized bilayer-couple model and the transition between oblate and prolate axisymmetric shapes. *Phys. Rev. E* **48**, 3112–3123 https://doi.org/10.1103/physreve.48.3112
- 33 Miao, L., Seifert, U., Wortis, M. and Döbereiner, H.-G (1994) Budding transitions of fluid-bilayer vesicles: the effect of area-difference elasticity. *Phys. Rev. E* **49**, 5389–5407 https://doi.org/10.1103/physreve.49.5389
- 34 Morris, C.E. and Homann, U. (2001) Cell surface area regulation and membrane tension. *J. Membrane Biol.* **179**, 79–102 https://doi.org/10.1007/s002320010040
- 35 Elani, Y., Purushothaman, S., Booth, P.J., Seddon, J.M., Brooks, N.J., Law, R.V. et al. (2015) Measurements of the effect of membrane asymmetry on the mechanical properties of lipid bilayers. *Chem. Commun.* **51**, 6976–6979 https://doi.org/10.1039/C5CC00712G
- Venable, R.M., Brown, F.L.H. and Pastor, R.W. (2015) Mechanical properties of lipid bilayers from molecular dynamics simulation. *Chem. Phys. Lipids* **192**, 60–74 https://doi.org/10.1016/j.chemphyslip.2015.07.014
- 37 Olbrich, K., Rawicz, W., Needham, D. and Evans, E. (2000) Water permeability and mechanical strength of polyunsaturated lipid bilayers. *Biophys. J.* **79**, 321–327 https://doi.org/10.1016/S0006-3495(00)76294-1
- 38 Sreekumari, A. and Lipowsky, R. (2022) Large stress asymmetries of lipid bilayers and nanovesicles generate lipid flip-flops and bilayer instabilities. *Soft Matter* **18**, 6066–6078 https://doi.org/10.1039/D2SM00618A
- 39 Brochard, F. and Lennon, J.F. (1975) Frequency spectrum of the flicker phenomenon in erythrocytes. J. Phys. 36, 1035–1047 https://doi.org/10.1051/iphys:0197500360110103500
- 40 Hochmuth, R.M. (2000) Micropipette aspiration of living cells. J. Biomech. 33, 15–22 https://doi.org/10.1016/S0021-9290(99)00175-X
- 41 Fin, A., Jentzsch, A.V., Sakai, N. and Matile, S. (2012) Oligothiophene amphiphiles as planarizable and polarizable fluorescent membrane probes. *Angew. Chem.* **124**, 12908–12911 https://doi.org/10.1002/anie.201206446
- 42 Dal Molin, M., Verolet, Q., Colom, A., Letrun, R., Derivery, E., Gonzalez-Gaitan, M. et al. (2015) Fluorescent flippers for mechanosensitive membrane probes. *J. Am. Chem. Soc.* **137**, 568–571 https://doi.org/10.1021/ja5107018
- 43 Colom, A., Derivery, E., Soleimanpour, S., Tomba, C., Dal Molin, M., Sakai, N. et al. (2018) A fluorescent membrane tension probe. *Nat. Chem.* **10**, 1118–1125 https://doi.org/10.1038/s41557-018-0127-3
- 44 Hjort Ipsen, J., Karlström, G., Mourtisen, O.G., Wennerström, H. and Zuckermann, M.J. (1987) Phase equilibria in the phosphatidylcholine-cholesterol system. *Biochim. Biophys. Acta* **905**, 162–172 https://doi.org/10.1016/0005-2736(87)90020-4
- 45 Veatch, S.L. and Keller, S.L. (2003) Separation of liquid phases in giant vesicles of ternary mixtures of phospholipids and cholesterol. *Biophys. J.* **85**, 3074–3083 https://doi.org/10.1016/S0006-3495(03)74726-2
- 46 Bagatolli, L.A. (2006) To see or not to see: lateral organization of biological membranes and fluorescence microscopy. *Biochim. Biophys. Acta* **1758**, 1541–1556 https://doi.org/10.1016/j.bbamem.2006.05.019
- 47 Foley, S.L., Hossein, A. and Deserno, M. (2022) Fluid—gel coexistence in lipid membranes under differential stress. *Biophys. J.* **121**, 2997–3009 https://doi.org/10.1016/j.bpj.2022.07.021
- 48 Nagle, J.F., Zhang, R., Tristram-Nagle, S., Sun, W., Petrache, H.I. and Suter, R.M. (1996) X-ray structure determination of fully hydrated L_{α} phase dipalmitoylphosphatidylcholine bilayers. *Biophys. J.* **70**, 1419–1431 https://doi.org/10.1016/S0006-3495(96)79701-1
- 49 Grabielle-Madelmont, C. and Perron, R. (1983) Calorimetric studies on phospholipid—water systems: I. dl-dipalmitoylphosphatidylcholine (DPPC)—water system. *J. Colloid Interface Sci.* **95**, 471–482 https://doi.org/10.1016/0021-9797(83)90207-2
- 50 Rawicz, W., Olbrich, K.C., McIntosh, T., Needham, D. and Evans, E. (2000) Effect of chain length and unsaturation on elasticity of lipid bilayers. *Biophys. J.* **79**, 328–339 https://doi.org/10.1016/S0006-3495(00)76295-3
- 51 Chen, D. and Santore, M.M. (2014) Large effect of membrane tension on the fluid–solid phase transitions of two-component phosphatidylcholine vesicles. *Proc. Natl Acad. Sci. U.S.A.* **111**, 179–184 https://doi.org/10.1073/pnas.1314993111
- 52 Portet, T., Gordon, S.E. and Keller, S.L. (2012) Increasing membrane tension decreases miscibility temperatures; an experimental demonstration via micropipette aspiration. *Biophys. J.* **103**, L35–L37 https://doi.org/10.1016/j.bpj.2012.08.061



- 53 Williamson, J.J. and Olmsted, P.D. (2015) Registered and antiregistered phase separation of mixed amphiphilic bilayers. *Biophys. J.* **108**, 1963–1976 https://doi.org/10.1016/j.bpj.2015.03.016
- Wagner, A.J., Loew, S. and May, S. (2007) Influence of monolayer–monolayer coupling on the phase behavior of a fluid lipid bilayer. Biophys. J. 93, 4268–4277 https://doi.org/10.1529/biophysj.107.115675
- Putzel, G.G. and Schick, M. (2008) Phase behavior of a model bilayer membrane with coupled leaves. *Biophys. J.* 94, 869–877 https://doi.org/10.1529/biophysi.107.116251
- 56 McConnell, H.M. and Kornberg, R.D. (1971) Inside-outside transitions of phospholipids in vesicle membranes. *Biochemistry* 10, 1111–1120 https://doi.org/10.1021/bi00783a003
- 57 Zachowski, A. and Devaux, Ph.F. (1990) Transmembrane movements of lipids. Experientia 46, 644–656 https://doi.org/10.1007/BF01939703
- 58 Nes, W.D. (2011) Biosynthesis of cholesterol and other sterols. Chem. Rev. 111, 6423–6451 https://doi.org/10.1021/cr200021m
- Hamilton, J.A. (2003) Fast flip-flop of cholesterol and fatty acids in membranes: implications for membrane transport proteins. Curr. Opin. Lipidol. 14, 263–271 https://doi.org/10.1097/00041433-200306000-00006
- 60 Leventis, R. and Silvius, J.R. (2001) Use of cyclodextrins to monitor transbilayer movement and differential lipid affinities of cholesterol. *Biophys. J.* 81, 2257–2267 https://doi.org/10.1016/S0006-3495(01)75873-0
- Drew Bennett, W.F., MacCallum, J.L., Hinner, M.J., Marrink, S.J. and Peter Tieleman, D. (2009) Molecular view of cholesterol flip-flop and chemical potential in different membrane environments. J. Am. Chem. Soc. 131, 12714–12720 https://doi.org/10.1021/ja903529f
- 62 Gu, R.-X., Baoukina, S. and Peter Tieleman, D. (2019) Cholesterol flip-flop in heterogeneous membranes. *J. Chem. Theory Comput.* **15**, 2064–2070 https://doi.org/10.1021/acs.ictc.8b00933
- Miettinen, M.S. and Lipowsky, R. (2019) Bilayer membranes with frequent flip-flops have tensionless leaflets. Nano Lett. 19, 5011–5016 https://doi.org/10.1021/acs.nanolett.9b01239
- 64 Hill, T.L. (1986) An Introduction to Statistical Thermodynamics, Dover, New York, NY
- 65 Doktorova, M., Symons, J.L., Levental, K.R., Lyman, E.R. and Levental, I. (2021) Challenging the dogma-cell plasma membranes are asymmetric not only in phospholipid composition but also abundance. *Biophys. J.* 120, 147a https://doi.org/10.1016/j.bpj.2020.11.1079
- 66 Symons, J.L., Doktorova, M., Levental, K.R. and Levental, I. (2022) Challenging old dogma with new tech: asymmetry of lipid abundances within the plasma membrane. *Biophys. J.* **121**, 289a–290a https://doi.org/10.1016/j.bpj.2021.11.1300
- 67 Leeb, F. and Maibaum, L. (2018) Spatially resolving the condensing effect of cholesterol in lipid bilayers. *Biophys. J.* 115, 2179–2188 https://doi.org/10.1016/j.bpj.2018.10.024
- 68 Tsamaloukas, A., Szadkowska, H. and Heerklotz, H. (2006) Thermodynamic comparison of the interactions of cholesterol with unsaturated phospholipid and sphingomyelins. *Biophys. J.* 90, 4479–4487 https://doi.org/10.1529/biophysj.105.080127
- 69 Huang, J., Buboltz, J.T. and Feigenson, G.W. (1999) Maximum solubility of cholesterol in phosphatidylcholine and phosphatidylethanolamine bilayers. Biochim. Biophys. Acta (BBA)—Biomembranes 1417, 89–100 https://doi.org/10.1016/S0005-2736(98)00260-0
- 70 Lu, L., Doak, W.J., Schertzer, J.W. and Chiarot, P.R. (2016) Membrane mechanical properties of synthetic asymmetric phospholipid vesicles. Soft Matter 12, 7521–7528 https://doi.org/10.1039/C6SM01349J
- 71 Karamdad, K., Law, R.V., Seddon, J.M., Brooks, N.J. and Ces, O. (2016) Studying the effects of asymmetry on the bending rigidity of lipid membranes formed by microfluidics. *Chem. Commun.* **52**, 5277–5280 https://doi.org/10.1039/c5cc10307j
- 72 Eicher, B., Marquardt, D., Heberle, F.A., Letofsky-Papst, I., Rechberger, G.N., Appavou, M.-S. et al. (2018) Intrinsic curvature-mediated transbilayer coupling in asymmetric lipid vesicles. *Biophys. J.* **114**, 146–157 https://doi.org/10.1016/j.bpj.2017.11.009
- 73 Kew, J.N.C. and Davies, C.H. (2010) Ion Channels: From Structure to Function, Oxford University Press, U.S.A.
- 74 Scott, H.L., Kennison, K.B., Enoki, T.A., Doktorova, M., Kinnun, J.J., Heberle, F.A. et al. (2021) Model membrane systems used to study plasma membrane lipid asymmetry. *Symmetry* **13**, 1356 https://doi.org/10.3390/sym13081356